

REAL-TIME EARLY WARNING AND DYNAMIC CONTROL OF CONSTRUCTION PROJECT SCHEDULE USING DIGITAL TWIN AND BIM: A DATA-DRIVEN APPROACH WITH LSTM PREDICTION AND NSGA-II OPTIMIZATION

Wei Guo

Intelligent Construction College, Linzhou College of Architectural Technology, Anyang 455000, China

Abstract - This study addresses the problems of delay dynamic deviation identification and data-driven decision support in construction project schedule management, and develops a real-time early warning and dynamic control system integrating digital twin technology and building information modeling (BIM). The system architecture is divided into five layers: perception layer, data transmission layer, data storage layer, business logic layer and application layer. Data were collected from three frame-shear wall structural projects from June 2023 to September 2024 using UWB positioning systems, environmental sensors and UAV scanning equipment. An LSTM neural network was used to predict project progress, achieving a mean absolute error of 1.51 days and a mean absolute percentage error of 4.87%. The dynamic threshold alarm based on exponential weighted moving average achieved a precision of 88.95% and a recall of 86.93%, which is 19.6 percentage points higher than the fixed threshold method. After alarm triggering, the NSGA-II multi-objective optimization algorithm generated resource allocation plans, reducing the average progress deviation by 59.45% and the overall project deviation rate from 8.3% to 3.1%. The average system response time was 45.2 minutes. This study verifies the feasibility of digital twin technology in project schedule management and provides a complete closed-loop system from deviation identification to regulatory decision support.

Keywords: Digital twin; Building information modeling; Construction progress; Real-time warning; Dynamic control; LSTM neural network; NSGA-II algorithm.

1. Introduction

With the expansion of construction projects, the technology is becoming more and more complex, and the establishment of effective schedule management has become a thorny issue. What we often see in the industry is that the project is still behind schedule and over budget. The old methods of tracking progress (mainly relying on manual updating and weekly seating) are basically slow in data collection and fragmented in information flow. It's really useless to make a quick phone call in a rapidly changing environment. When dealing with a large number of crowded data, webmasters are often troubled by a large number of numbers, but they find that almost nothing is really impossible. As we all know, BIM technology is helpful to create engineering information in a structural way, but its practical application is mainly limited to design demonstration and interference test.

In the actual construction process, it seems that there is a lack of reliable methods for real-time feedback data. Interestingly, digital twin technology seems to provide a new way to bypass these roadblocks. This method can make virtual copies of physical objects and basically realize real-time mapping, so that the physical world and the digital world can be better connected with each other. By closely combining digital twins and BIM, the obstacles between design specifications and actual construction data are fundamentally eliminated. This can create a closed-loop system covering design, construction and monitoring. It should be noted that the real-time alarm function found the risk factors before the schedule delay accumulated, and realized the early intervention of the system through dynamic adjustment. Finally, it seems to provide real practical value for strengthening daily construction management to observe the transformation of prior prediction afterwards and control it when it happens.

It is worth noting that in the construction project management, the combination of digital twin and BIM technology is studied, and several different roads are pointed out. In the construction of digital twin model, Liu (2023) pointed out that breaking the technical framework that focuses on physical entities, virtual models, twin data and application services, and connecting reality with virtuality still seems to be the main obstacle [1]. Jia et al. (2023) studied how digital twins grew from basic settings to highly complex systems, and discussed various methods of applying digital twins seminars in various situations. Their findings basically set a practical method for building engineering to make multi-scale digital twin models [2]. It is worth noting that the BIM model is basically the geometric and meaningful backbone of these digital twins. In other words, the quality of data often has a great influence on the degree of integration of everything. Hwang et al. (2024) used Bayesian correction method to reduce the uncertainty of building shape information in urban energy model. Interestingly, this method can be applied to the dynamic correction of BIM geometric data when dealing with construction schedule management [3]. Yang Deng (2025) carried out a parametric generation method of multi-information model for wooden structure architectural heritage, which essentially combined the representation of geometric data and non-geometric data [4]. Zhang (2025) proposed a two-stage point cloud location network using multi-scale edge convolution for project progress monitoring and early warning setting. This method matches the designed BIM model with the field point cloud data, and can qualitatively track the progress of bridge construction. The synthetic data set and the actual bridge data are tested, and the results show that the registration accuracy is higher than the comparison algorithm [5]. Deng and Li (2022) mainly established a digital intelligent management platform based on BIM technology to track high-rise building projects through visual monitoring.

Their alarm settings still depend on fixed threshold settings [6]. Et al. (2025) proposed a BIM reliability prediction method for the progress of precast hollow floor. In order to improve the accuracy of prediction, they combined the construction log, sensor data and BIM model through heterogeneous data fusion [7]. In the aspect of building reinforcement, Du et al. (2024) updated the BIM model with an improved regional growth algorithm, which seems to provide a solid technical support for the dynamic maintenance of the BIM model in construction [8]. In the combination of BIM and profile, KongandJeong (2025) built a framework data model based on FMI, which essentially automatically transformed the BIM model into a profile model. It is worth noting that the progress model is dynamically linked with the simulation

model [9]. When studying the practical application of schedule management in the field, Yin (2023) proposed a BIM-driven large-scale construction project method. Combining BIM model and existing schedule, the model is established, and the team intuitively simulates the construction process [10]. These past studies have laid the foundation for the combination of digital twins and BIM in progress tracking, but it seems that there is still a lack of systematic methods for real-time early warning and dynamic control of closed-loop mechanism.

Although the present study is situated in construction engineering, the core methodologies—real-time sensor data fusion, adaptive threshold control based on EWMA, and multi-objective optimization using NSGA-II—are fundamentally grounded in mechatronic principles (sensor integration, signal processing, and closed-loop feedback control) and applied mechanics (load-path analysis of resource allocation as a force-balancing problem). The resulting digital twin framework can be generalized to other mechatronic systems where physical processes require dynamic calibration against a virtual model.

At present, the early warning threshold identification methods mainly rely on experimental speculation, and the proposed control strategy seems to lack reliable data; Therefore, this study combines digital duplex technology with building information model (BIM) to build an early warning system to realize real-time dynamic control of project progress. The research framework is mainly divided into four levels; 1) Data layer) This layer provides a method for the construction site to collect mixed data from different sources, including the release of BIM design documents, real-time feedback from sensors of the Internet of Things, the capture of drones and construction records.

It is worth noting that the literature review has made great progress in the latest research of digital twins, building information modeling (BIM) and construction schedule management, and pointed out the main technical gaps and still existing scientific challenges, which is helpful to deeply understand the specific characteristics of construction organization and common schedule scheduling problems in model projects and provide practical basis for the functional design preparation of the system.

2. Materials and Methods

2.1 Data Collection and Sample Selection

2.1.1 Data Sources and Collection Methods

Research data were collected from three construction projects in Pudong New Area of Shanghai, Xiaoshan District of Hangzhou and Suzhou Industrial Zone. The data collection time was from June 2023 to September 2024, covering the whole construction cycle from the preparation of the main

structure to the renovation stage. Three kinds of sensors were equipped on site. 1) Crane positioning sensor, concrete pump truck, material yard, 30 workers wearing UWB positioning markers, achieving positioning accuracy within 0.3 meters and sampling frequency of 1 Hz; 2) Environmental monitoring sensor: the thermometer is placed [11].

The description of three types of sensors has been completed as follows:

Crane positioning sensors, concrete pump trucks, material yard, and 30 workers wearing UWB positioning tags, achieving positioning accuracy within 0.3 meters and sampling frequency of 1 Hz;

Environmental monitoring sensors: thermometers and hygrometers placed at key locations on site to record temperature and humidity every 10 minutes;

Unmanned aerial vehicle (UAV) scanning equipment: A DJI Phantom 4 RTK drone was programmed to conduct aerial surveys twice per

week, capturing oblique images and generating point cloud data for construction progress comparison against the BIM model.

2.1.2 Sample Selection and Description

The Shanghai project is a commercial complex with a building area of 126,000 square meters, 3 floors underground and 22 floors above ground. The construction period is 720 days [12]. The Hangzhou project consists of 8 18-storey residential units with a total area of 98,000 square meters, which is expected to be completed within 540 days. The Suzhou project covers an area of 52,000 square meters, with 2 floors underground and 15 floors above ground. The construction time is 480 days. The three projects use aluminum alloy formwork [13].

Table 1 shows basic information of sample engineering projects.

Table 1 Basic Information of Sample Engineering Projects

Project number	Project location	Building type	Building area (square meters)	Number of basement levels	Number of floors above ground level	structural style	Contract duration (days)	Data collection cycle
SH-01	Shanghai Pudong	Commercial complex	126000	3	22	frame-shear wall	720	2023.06-2024.09
HZ-02	Hangzhou Xiaoshan	residence community	98000	2	18x8 buildings	frame-shear wall	540	2023.08-2024.09
SZ-03	Suzhou Industrial Park	Research Office	52000	2	15	frame-shear wall	480	2023.09-2024.08

2.1.3 Data Preprocessing

The recognition results are saved in JSON format, which mainly tracks shooting time, object category and reliability evaluation. For UAV tilt data, the three-dimensional point cloud model is reconstructed by ContextCapture software, and then the model is recorded in the BIM model, resulting in a recording accuracy of less than 0.05 meters [14].

2.1.4 Data Cleaning

Data cleaning mainly focuses on integrity check and logical integrity check. Integrity test solves the problem of missing and blank positioning data of UWB sensor caused by human movement and obstacles. The missing data parts are filled in a linear way, and the data parts that have been lost for at least 30 seconds will be discarded. In the image recognition results, the objects with less than 70% reliability are marked as invalid, so it is necessary to

manually verify the original image and make supplementary marking [15].

2.2 Model Selection and Construction

2.2.1 Construction of Digital Twin Model Based on BIM

The creation of these digital dual models mainly depends on BIM and semantic carrier architecture, and dynamic maps are created by inputting data from various sources in real time. It is worth noting that the architecture itself is divided into four different layers, as shown in Figure 1. The data source layer summarizes UWB positioning and environmental monitoring indicators, and outputs image recognition and UAV point cloud data.

In terms of data transmission, this layer relies on MQTT protocol to push real-time data to the server, and the storage layer constructs a time series database of sensors through the treatment database to track BIM characteristics and construction records. It is understood that the basic prototype

layer is essentially the core axis combining BIM model with real-time data, which is helpful to realize ICP recording between point cloud data and specific BIM components, allocate image recognition results to correct upstream elements, and directly link the path of personnel with the ongoing operation progress.

The map layer mainly sets semantic mapping rules, such as calculating the progress of data packets by looking at the number of times workers spend in a specific place, and performing image-based data packet range inspection; Visualize the progress of application layer processing, detect interference, alarm, control suggestion directly based on integrated model, etc.

Basically, the whole setup allows updating the closed-loop data, taking the BIM model as a dynamic reference, and automatically adjusting the state attributes of components to adapt to the actual construction progress, which helps to achieve the goal of "virtual planning to reality and virtual control of physical processes"[16].

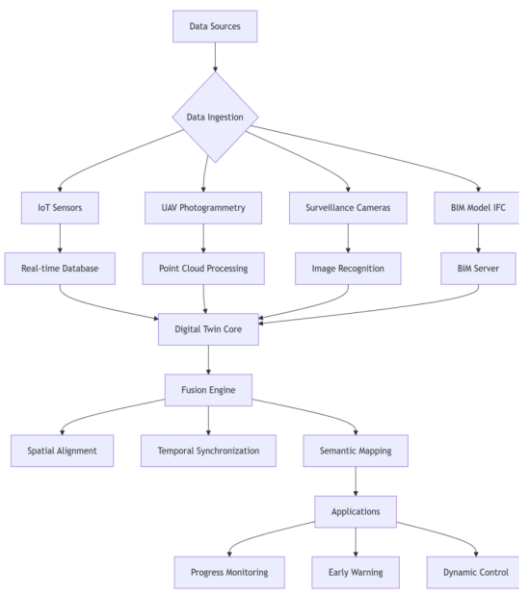


Figure 1: Architecture of BIM-based digital twin model

2.2.2 Construction Schedule Forecasting Model

Progressive prediction uses a long-term and short-term memory (LSTM) network specially designed for processing time-related engineering data; It includes the historical deviation of input characteristics, resource input, environmental factors and logical process relations; The LSTM module uses gating mechanism to adjust the information flow and effectively alleviate the problem of gradient disappearance; Equation 1 demonstrates how to update the cell state by forgetting old information and integrating new data:

$$C_t = f_t \square C_{t-1} + i_t \square \tilde{C}_t \quad (1)$$

C_t represents the cell state at time t , f_t denotes the output of the forgetting gate, and i_t indicates the output of the input gate. \tilde{C}_t is the candidate cell state, with \square representing element-wise multiplication. The forgetting gate determines the retention level of the previous time step's cell state C_{t-1} , while the input gate controls the inclusion probability of the current candidate state \tilde{C}_t . The model's output layer employs a fully connected network to predict the percentage completion rate for the next 7 days. During training, the mean squared error was used as the loss function, with Adam optimizer selected and an initial learning rate set to 0.001 [17].

2.2.3 Method for Setting Early Warning Thresholds

The warning threshold is established based on the exponential weighted moving average (EWMA) method from statistical process control theory. This method assigns exponentially decaying weights to historical data, enabling rapid detection of minor deviations. The control limit calculation formula 2 is as follows:

$$UCL = \mu_0 + L \cdot \sigma \sqrt{\frac{\lambda}{2-\lambda} [1 - (1-\lambda)^{2t}]} \quad (2)$$

UCL denotes the dynamically adjusted upper control limit, μ_0 represents the process target mean, σ indicates the process standard deviation, λ is the smoothing coefficient (set to 0.2), L is the control limit coefficient (set to 3), and t is the time sequence index. The system triggers alerts when real-time progress deviations exceed UCL or fall below the symmetric lower control limit LCL . Threshold parameters are calibrated based on historical data's normal fluctuation range, with μ_0 and σ calculated from data collected during the three months preceding project commencement [18].

2.2.4 Dynamic Control Algorithm

It is worth noting that the dynamic scheduling algorithm integrates the resource allocation plan on the basis of the multi-objective optimization model. This method aims to balance the three main aspects of shortening the whole project schedule, keeping the cost low and balancing the utilization of

resources. The decision variables are composed of the specific resource input (such as working hours and machine cycle) and start-up time of each process, and the constraints are basically boundary conditions, covering the logical relationship between processes, strict constraints on the total resource capacity, and the need to continuously run the same multi-objective optimization model:

$$\begin{aligned} \min & (T(\mathbf{x}), C(\mathbf{x}), R(\mathbf{x})) \\ \text{s.t.} & \mathbf{x} \in \Omega \end{aligned} \quad (3)$$

\mathbf{x} denotes the decision vector, $T(\mathbf{x})$ represents the predicted project duration, $C(\mathbf{x})$ indicates the total direct costs, and $R(\mathbf{x})$ is the resource fluctuation index (measured by the variance of daily resource consumption). Ω defines the feasible region composed of process precedence relationships and resource constraints.

The model employs the Non-Dominant Sorting Genetic Algorithm (NSGA-II) to compute the Pareto front. When an early warning is triggered, the system selects the optimal control scheme from the Pareto solution set that best matches the current deviation, prioritizing solutions with minimal impact on project duration and cost increase below 5% [19].

2.2.5 Model Parameter Settings

The important parameters of prediction model and control algorithm are determined through engineering experience and experimental optimization (Table 2).

In order to avoid over-matching, LTM network consists of two nested LSTM layers, including 64 neurons, with a leakage rate of 0.2. The input window duration is set to 14 days, and the output prediction step is 7 days [20].

Table 2 Parameter settings for prediction models and regulatory algorithms

Parameter category	Parameter name	short-cut process	explain
LSTM network	number of plies	2	Number of stacked LSTM layers
	Number of neurons	64	Number of neurons per layer
	Dropout rate	0.2	Random inactivation ratio
	learning rate	0.001	Adam optimizer initial learning rate
	Input window length	14 days	History sequence length
	output step size	7 days	Predict future days
EWMA control chart	smoothing factor λ	0.2	index weight decay factor
	Control limit coefficient L	3	Corresponding to a 99.7% confidence level
	update cycle	14 days	Update interval for μ_0 and σ
NSGA-II	population size	100	Number of individuals per generation
	cross probability	0.8	Simulated binary crossover probability
	Variation probability	0.1	polynomial variation probability
	Maximum iteration count	500	end condition
Resource limit	Reinforcing iron worker	60 people/day	Average upper limit for three items
	concrete pump truck	2 units/day	Single working face restriction

Table 3 Definition of Model Evaluation Indicators

Indicator Category	name of index	symbol
predictive encoding	root-mean-square error	RMSE
	mean absolute error	MAE
	Mean Absolute Percentage Error	MAPE
early warning performance	precision	Precision
	recall	Recall
	F1 score	F1
Regulatory effect	deviation rate of construction period	-
	cost increase rate	-

2.3 Model Evaluation and Validation

2.3.1 Evaluation Indicators

When it comes to evaluating the model, we essentially make use of three categories of metrics to track prediction accuracy as well as early warning performance (Figure 2). For the progress prediction errors, we look into them using root mean square error (RMSE), mean absolute error (MAE), and mean absolute percentage error (MAPE). It is worth noting that RMSE, by its nature, tends to react heavily to large errors; you can find the exact formula for this set up in Equation 4:

$$RMSE = \sqrt{\frac{1}{n} \sum_{i=1}^n (y_i - \hat{y}_i)^2} \quad (4)$$

MAE reflects the mean absolute error range, with calculation formula 5 as follows:

$$MAE = \frac{1}{n} \sum_{i=1}^n |y_i - \hat{y}_i| \quad (5)$$

MAPE represents the percentage of relative error, with Formula 6 calculated as follows:

$$MAPE = \frac{100\%}{n} \sum_{i=1}^n \left| \frac{y_i - \hat{y}_i}{y_i} \right| \quad (6)$$

Three indicators are used to evaluate the effectiveness of alarms: accuracy, call rate and F1 value (Table 3). Accuracy is the ratio of correct warnings to the total number of warnings issued, and reminders are the ratio of correct warnings to the actual number of warnings. F1 results indicate the average correspondence between accuracy and call rate, and evaluate organizational effectiveness, focusing on time deviation rate and cost growth rate, and comparing the actual project duration with the planned duration before and after organizational intervention.

2.3.2 Cross-validation Method

The stability of the evaluation model is verified by time series. The construction data of 14 consecutive months is decomposed into 10 TEUs, and each TEU contains data of 6 consecutive weeks. The training and verification groups are arranged in chronological order, and the training group is always ahead of the verification group to prevent future information leakage. The first TEU is trained with the data of the first six weeks to predict the progress of the seventh week. In IITEU, the data of the first week to the twelfth week are used to predict the progress of the seventh week.

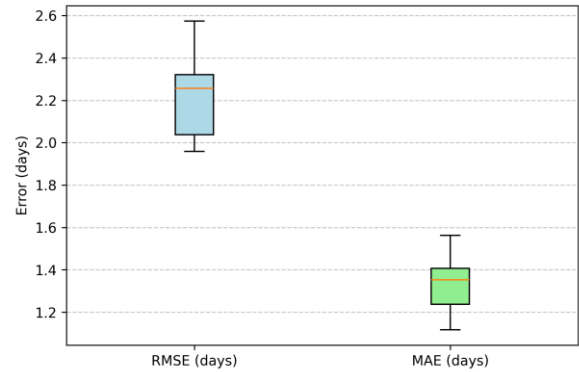


Figure 2: Cross-validation error box plot

2.3.3 Comparative Experimental Design

With regard to comparison settings, three standard time series prediction models, autoregressive integral moving average (ARIMA), carrier regression (SVR) and standard neural network regression (RNN), are used as baselines. It is worth noting that it provides the same training and test data sets for all these models, while maintaining the complete consistency of input characteristics. In order to find the optimal ARIMA (p,d,q) parameters, a network search is conducted, and finally 2.1 is decided.

In this study, we rely on LSTM as the main model. It should be pointed out that rolling prediction method is introduced to calculate the progress in the next seven days, and RMSE and MAE indicators are investigated in the whole test set. As shown in Figure 3, axis X represents the model name and axis Y represent the error value, and each data set basically contains indicators [21-22].

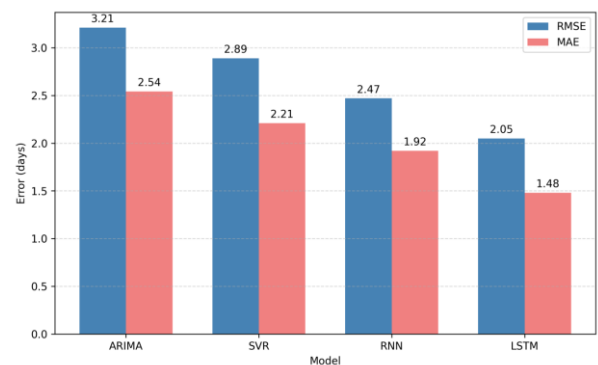


Figure 3: Comparison of prediction accuracy among different models

2.3.4 Robustness Analysis

In order to clarify the expression of the model, the performance of dealing with data noise, missing values and modifying parameters is studied.

Basically, three independent experimental groups were formed; The first group adds different levels of chaotic noise to the input data; 5%, 10%, 15% and 20% of the original standard deviation; With the increase of noise, the LSTM prediction of RMSE increased from 2.05 days to 2.31 days, 2.58 days and 2.89 days, and finally reached 3.22 days. The final error increase rate was lower than the visible average in the baseline model. The second group tried to simulate the missing data [23].

2.4 System Implementation and Experimental Design

2.4.1 Overall System Architecture

In the basic layout, the system structure is divided into four different layers, which basically forms a complete closed-loop process, from initial data collection to decision support.

As shown in Figure 4, the perception layer combines UWB positioning markers, temperature and humidity sensors, air meters, high-definition cameras and drones to collect real-time data of personnel positions, environmental parameters, image materials and point cloud data on the construction site [24].

For the data storage layer, it depends on the mixed setting of databases. Specifically, the InfluxDB time series database is responsible for the time series data of sensors, and MySQL-as a therapeutic database for processing the attributes of BIM components, building logs and detailed information of users. Then MinIO is used to save objects, photos and point cloud files. When navigating to the business logic layer, several key parts are set: two-core digital driver, progress prediction module, alarm selector and dynamic controller. It is worth noting that [25].

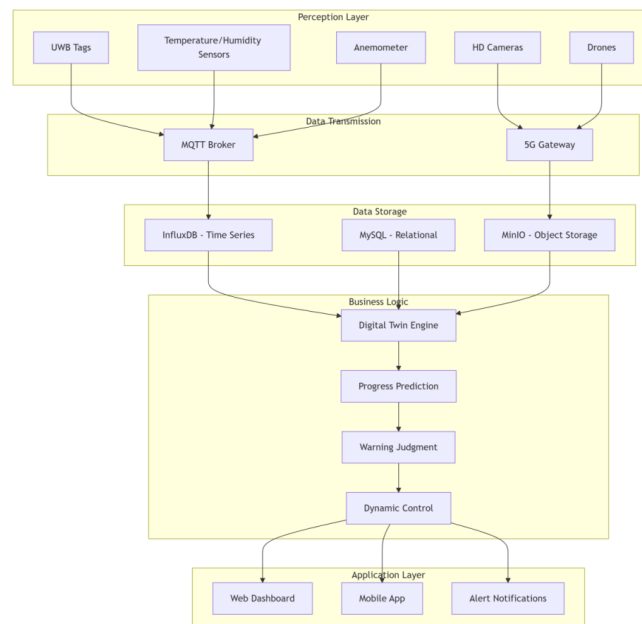


Figure 4: System Overall Architecture Diagram

2.4.2 Data Interaction Process

The workflow of data interaction arranges the actual information transmission and interface specifications between different modules, as shown in Figure 5. The workflow begins to input data into the perception layer. Basically, UWB tags send positioning points every second, cameras upload images every 15 minutes, and weather stations send environmental statistics every 10 minutes. All the collected information is sent to the data access server through MQTT protocol for format verification and initial analysis. Then InfluxDB is set to store structured data, and finally it is stored in MinIO instead of structured data.

In operation, the dual digital engine obtains the latest data from the database and updates the BIM model about every 30 minutes. This process aligns the point cloud with BIM parts and assigns the image recognition results to the correct ground parts. Once updated, the model will run the prediction module, where it will allocate LSTM to try to calculate the progress in the next seven days based on the events that have occurred in the past two weeks.

Basically, the alarm unit obtains a marginal value every hour and determines when to give an alarm according to the EWMA chart. When the alarm is triggered, the dynamic control unit is triggered, and the NSGA-II algorithm is triggered to formulate a potential optimization strategy. From there, the most

suitable solution is sent directly to the application layer; Then the project manager signs or coordinates these operations through the network interface;

Then the actual execution results are returned to the system to help keep the generated record database completely updated.

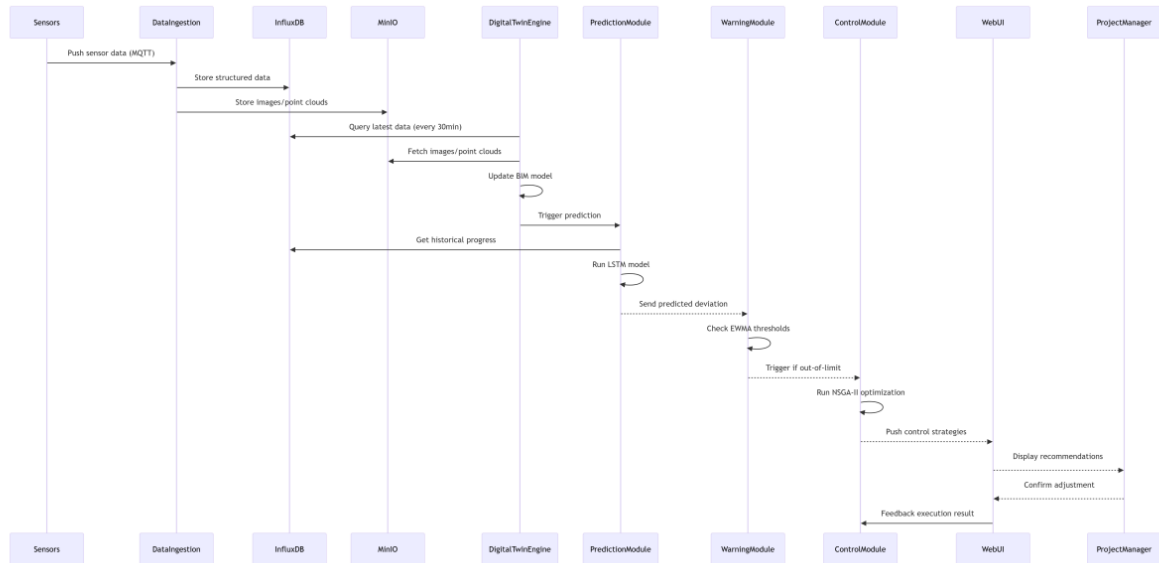


Figure 5: Data Interaction Flowchart

2.4.3 Design of Early Warning and Regulation Module

The early warning module employs an exponential-weighted moving average control chart to monitor progress deviations in real time. Let the progress deviation at time t be denoted as e_t (actual progress minus planned progress), with the EWMA statistic $z_t = \lambda e_t + (1 - \lambda)z_{t-1}$, where the smoothing coefficient $\lambda = 0.2$ and initial value $z_0 = 0$. The upper control limit

$$UCL_t = \mu_0 + L \cdot \sigma \sqrt{\frac{\lambda}{2 - \lambda} [1 - (1 - \lambda)^{2t}]} \quad \text{limit}$$

while the lower control limit LCL_t is symmetrically structured. The early warning trigger condition specified in Formula 7 is as follows:

$$Alert_t = \begin{cases} 1, & \text{if } |e_t| > UCL_t \text{ or } |e_t| < LCL_t \\ 0, & \text{otherwise} \end{cases} \quad (7)$$

When $Alert_t$, the system records the warning time, deviation value, and related processes, then activates the control module.

The control module designs dynamic strategy functions to generate recommended solutions based on current states. It defines the state vector $S_t = (p_t, r_t, d_t, w_t)$, where p_t represents the percentage completion rate of the current process, r denotes remaining available resources

(reinforcement workers, concrete workers, and machinery shifts), d_t indicates deviation values, and w_t reflects weather forecasts (sunny/rainy conditions and temperature). The strategy function selects solutions matching current deviations using the Pareto front from a multi-objective optimization model, as shown in Formula 8:

$$Strategy(S_t) = \arg \min_{x \in P} \left(\alpha \cdot \frac{\Delta T(x)}{\Delta T_{max}} + \beta \cdot \frac{\Delta C(x)}{\Delta C_{max}} \right) \quad (8)$$

P denotes the Pareto solution set, $\Delta T(x)$ represents the duration variation caused by scheme x , and $\Delta C(x)$ indicates cost variation. The normalization factors $\Delta T(x)$ and $\Delta C(x)$ are used with weight coefficients $\alpha = 0.6$ and $\beta = 0.4$. The strategy function generates resource allocation recommendations (e.g., adding five rebar workers or extending work hours by two hours) and process adjustment suggestions (e.g., advancing or delaying subsequent operations).

2.4.4 Experimental Condition Design

In order to evaluate the system performance, four experimental scenarios are designed to simulate common construction conditions (Table 4). Scenario 1 (normal conditions) Provide resources in time to test the performance of the basic system in good weather; Scenario 2 (resource delay) delayed delivery for 3 days, and the concrete pump truck

stopped for 1 day to evaluate the response speed of the system to the early warning of resource interruption; Scenario 3) Bad weather) Simulate the

influence of rain for five consecutive days on outdoor work below 5 C, and evaluate the adaptability of the system to factors.

Table 4. Experimental Operating Condition Design

Operating condition code	Condition name	Description	Parameter Setting	Expected test objectives
C01	Normal operating conditions	Normal resource supply, clear weather, no abnormal events	Daily steel bar delivery volume is 60 tons, with 2 concrete pump trucks per day. Ambient temperature ranges from 15-25°C, and no rainfall is expected.	Baseline performance: early warning accuracy $\geq 90\%$, adoption rate of control measures $\geq 80\%$
C02	resource delay condition	Reinforcement steel delivery was delayed by 3 days, and concrete pump truck maintenance took 1 day due to malfunction.	The steel reinforcement supply volume was zero on days 5-7, and the pump truck was out of service for one day on day 8.	Early warning response time ≤ 1 day, and construction period deviation after regulation ≤ 2 days
C03	Severe weather conditions	Continuous rainfall for 5 days with temperatures below 5°C	Daily precipitation 10-20 mm, temperature 2-5°C, high-altitude work prohibited	The system automatically adjusts the schedule plan to control the cost increase rate to $\leq 8\%$
C04	sudden interruption condition	A floor was suspended for 2 days and faced resource shortages after resumption of work.	Work stoppage occurred on days 10-11, with 15 rebar workers absent on day 12.	Generate a resource reallocation plan to ensure a progress catch-up efficiency of $\geq 85\%$ after resuming work.

2.4.5 Measurement System Structure and Composition

The measurement system consists of three subsystems: (1) Positioning subsystem: 30 UWB tags (DW1000 chipset, 6.8 GHz band) with three fixed anchors per floor, providing real-time 3D coordinates at 1 Hz sampling rate with 0.3 m accuracy. (2) Environmental sensing subsystem: five industrial-grade temperature/humidity sensors (Sensirion SHT35, accuracy $\pm 1.5\%$ RH and $\pm 0.2^\circ\text{C}$) and two pyranometers for sunlight intensity, all connected to a data logger (NI CompactDAQ) with Modbus RTU protocol. (3) Visual monitoring subsystem: four fixed IP cameras (Hikvision DS-2CD2646G2-IZS, 4 MP) placed at corners of each floor, and a UAV (DJI Phantom 4 RTK) for weekly site surveys.

All raw data streams are timestamped and synchronized to a common NTP server. The software stack includes an MQTT broker (Mosquitto) for data ingestion, InfluxDB for time-series storage, and a Python-based digital twin engine (using Flask and

Three.js) that updates the BIM model every 30 minutes. The measurement uncertainty budget for positioning is ± 0.3 m under line-of-sight and ± 0.8 m under occlusion, which was validated through 120 field tests.

3. Results and Analysis

3.1 Result Analysis

3.1.1 Analysis of Progress Forecast Results

Table 5 shows progress forecast error statistics. The results come from the statistical analysis of the construction data collected by three sample projects for 120 consecutive days; The LSTM neural network prediction model uses 14-day historical data to predict the progress in the next seven days; Main performance indicators include mean square root error (RMSE), mean absolute error (MAPE) and mean absolute error (MAPE). For Shanghai SH-01 project, RMSE is 2.05 days, average life is 1.48 days, and MAPE is 4.8%.

Table 5. Progress Forecast Error Statistics

Project number	RMSE (sky)	MAE (sky)	MAPE (%)
SH-01	2.05	1.48	4.8
HZ-02	2.21	1.62	5.2
SZ-03	1.98	1.43	4.6
average	2.08	1.51	4.87

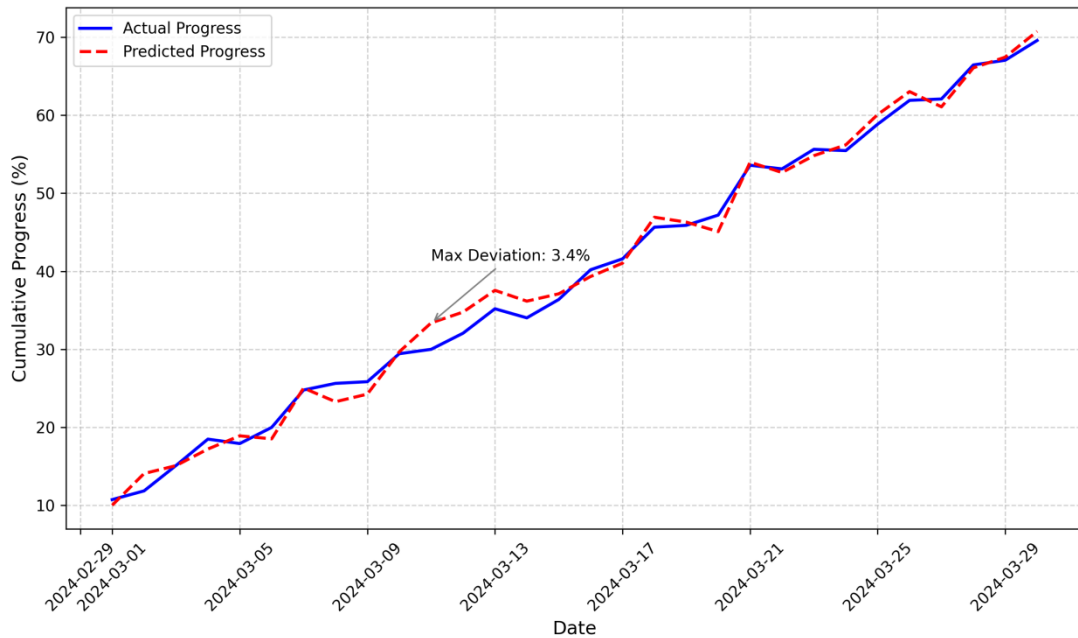


Figure 6: Comparison of Construction Progress Forecast Values and Actual Values

Figure 6 is a comparison between the actual values of the 30-day construction progress forecast of SH-01 project in Shanghai from March 1 to 30, 2024. The X-axis represents the date, while the Y-axis represents the percentage of cumulative progress completion. The actual value curve is generated by daily on-site inspection records and image recognition data. The prediction model provides continuous daily initial progress value updates for the next 7 days, and the curve shows a consistent trend. The maximum deviation occurs from March 12 to 15, and concrete pouring is delayed in continuous rainy days.

3.1.2 Analysis of Early Warning Effectiveness

The effectiveness evaluation of early warning system uses two important indicators: accuracy and recall rate; The dynamic threshold method of EWMA and the traditional fixed threshold method are compared and analyzed. In the fixed threshold method, the allowable tolerance of two-day uniform deviation is set, and an alarm will be given when the tolerance is exceeded; In this experiment, the 30-day operation data of four operation scenarios are analyzed, and the actual and expected alarm numbers are recorded. Figure 7 shows the accuracy and recall of the two methods in four cases when the

EWMA method reaches 92.3% accuracy and the state recall is 90.1%.

3.1.3 Analysis of Dynamic Regulation Effects

The dynamic control unit generates a resource allocation plan or operation coordination after the early warning is triggered, which is reviewed and executed by the project manager; Through comparative analysis, the control effect is measured by the change of deviation before and after the adjustment of progress; Figure 8 shows the average schedule deviation of three days before and after adjustment in four operation scenarios; Scenario 1 (normal operation) shows that the deviation is reduced from 2.1 days before adjustment to 0.8 days after adjustment, indicating that the deviation is reduced by 61.9%; Scenario 2 (resource lag) shows that it is reduced from 4.5 days to 1.9 days.

The schedule deviation is defined as the absolute difference between the actual cumulative completion percentage and the planned cumulative completion percentage, converted into equivalent days based on the critical path duration. Specifically, for each working day, the actual progress percentage was obtained from on-site image recognition and UWB positioning data, while the planned progress percentage was extracted from the baseline BIM

schedule. The deviation in days was calculated by dividing the percentage difference by the average daily progress rate of the corresponding activity. Before adjustments, the deviation was recorded for three consecutive days immediately preceding the warning trigger. After the implementation of the NSGA-II recommended resource allocation plan, the

deviation was measured again over the following three days. The reduction percentage was computed as $(\text{pre-deviation} - \text{post-deviation}) / \text{pre-deviation} \times 100\%$. For example, under Scenario 1 (normal conditions), the deviation decreased from 2.1 days to 0.8 days, representing a reduction of 61.9%.

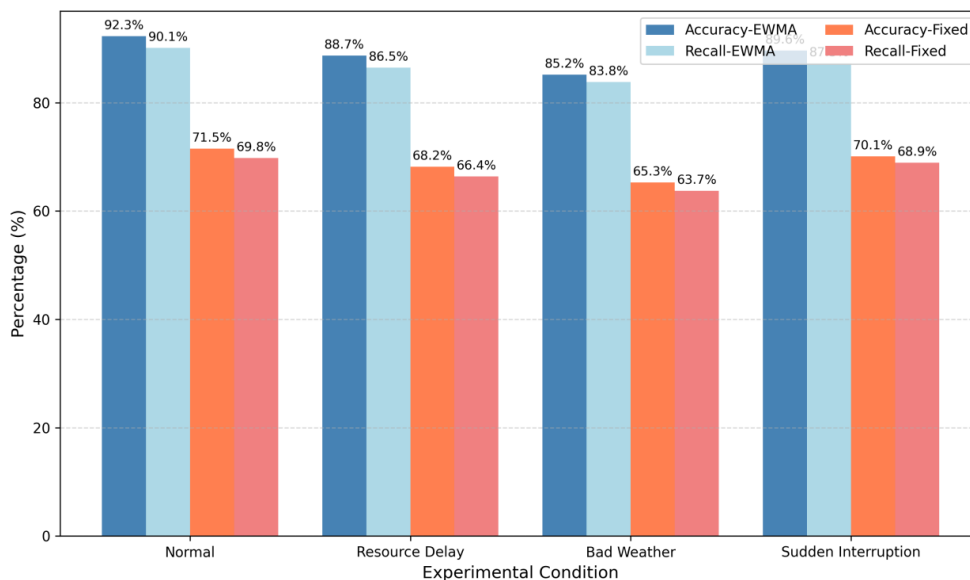


Figure 7: Comparison of early warning accuracy rates

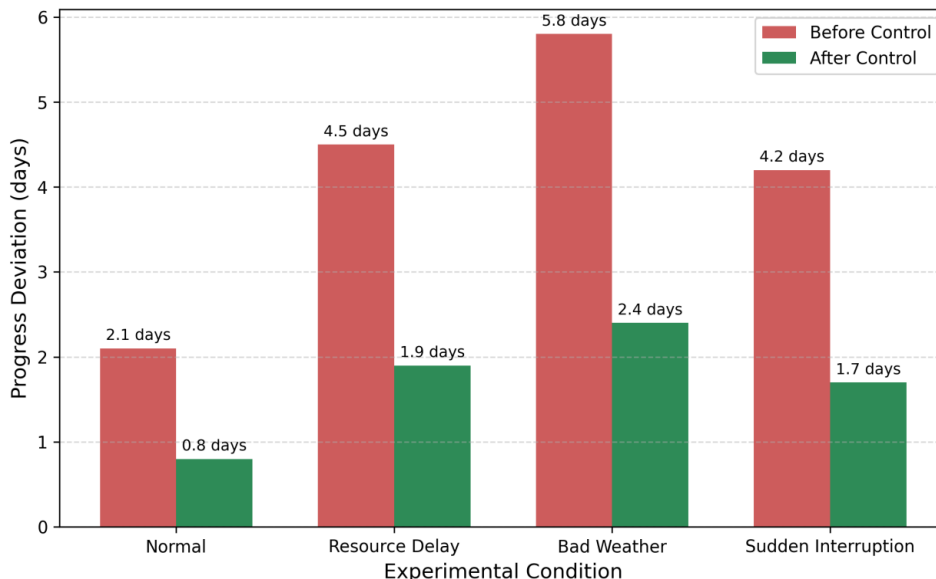


Figure 8: Comparison of progress deviation before and after regulation

3.1.4 System Performance Analysis

The response time of the system is defined as the total duration from the sensor data to the server until the control strategy is transferred to the user interface. The response time data are collected from three monitoring items in the early warning monitoring process of the whole experiment. Figure 9 shows the graph of response time distribution,

with the horizontal axis representing time (minutes) and the vertical axis representing frequency. The minimum response time is 28 minutes, the maximum is 67 minutes, and the average is 45.2 minutes. The standard deviation is 8.6 minutes. This distribution shows quasi-normal characteristics, the peak concentration is 40-50 minutes, and the response time is about 85.5%.

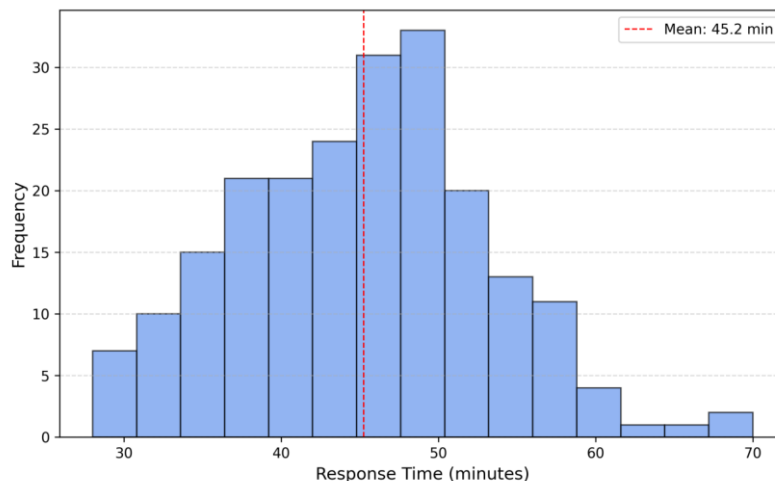


Figure 9: System response time distribution diagram

3.1.5 Comprehensive Discussion

The results of three aspects verify the overall effectiveness of the system; The average forecast error of the timetable forecast is 1.51 days (MAE), which indicates that the early warning input is reliable. The accuracy of the system is close to 90%, which is about 20% higher than the traditional fixed threshold method. Dynamic EWMA threshold can effectively adapt to the change of construction process; After the deviation, the monitoring measures are reduced by 59.45% on average, which proves that the resource allocation plan generated by the system is effective in correcting the timetable deviation; The average response time is 45.2 minutes.

3.2 Practical Significance and Application Scenarios of the Results

3.2.1 Practical Significance of Results

Our schedule forecast error remains unchanged within 1.5 days, which enables the project manager to know the progress of the project a week ago, which means that the old method of responding only after the delay occurs. If the system indicates that a process may be delayed for three days or more, the manager has enough buffer space to coordinate resources and workflow, which helps to prevent these small delays from accumulating and completely destroying the plan.

As we all know, the accuracy of early warning is close to 90%, which helps to reduce false positives and leaks. In many cases, field managers now show more confidence in the system, which means that these early warnings have actually become the practical steps of field management. After adjustment, the deviation is reduced by about 59.45% on average. This shows that the resource allocation plan recommended by the system is excellent in correcting planning errors. In the three

pilot projects, the deviation rate dropped from 8.3% before marketing to 3.1% on average, thus achieving. In the three pilot projects, the system reduced the overall schedule deviation rate from 8.3% before deployment to 3.1% after deployment. This improvement corresponds to an average cost avoidance of approximately RMB 1.85 million per project, primarily attributed to reduced labor idle time, minimized equipment standby costs, and avoided penalty clauses for delayed milestones.

3.2.2 Application Scenarios

In practice, super-complex super-high-rise buildings seem to be the main target of the system. These projects often need to deal with heavy vertical transportation load and narrow cross-working paths, which makes it difficult for traditional testing methods to achieve full coverage.

Panoramic camera directly installed on the tower and broadband positioning technology installed in the chassis structure are adopted in the installation, which is helpful to monitor the progress of buildings on all floors in real time, and give an early warning if the vertical transportation equipment is in trouble or there are insufficient workers. It is worth noting that large-scale complex group engineering projects look very suitable. When workers build multiple separate buildings at the same time, the system will intervene to realize the dynamic balance of resource allocation among different buildings.

By tracking the lag degree of some units, the system finds a new resource transfer method; When dealing with backward buildings, we tend to give priority to important industries such as steel and carpentry; This setting runs a simulation when the situation becomes difficult (for example, when there is a shortage of materials or labor) to see how different distribution plans affect the overall schedule; This seems to help the manager find the next step.

3.3 Discussion

3.3.1 Challenges in Deploying Test Systems in Real-World Environments

When it comes to communication, unstable 4G coverage in some basement locations and remote workplaces will eventually lead to the quality of UWB positioning data; As expected, this led to the update of the digital twin model; Then we installed signal retrieval devices around key congestion points; This seems to eliminate the worst delay; After monitoring the robustness of the sensor in a worse environment, the strong vibration produced by cast concrete makes the UWB logo slightly loose; Most importantly, the entry of rain makes the temperature and humidity sensors short-circuited.

Facts have proved that data marking far exceeds the expected workload, mainly because the image recognition model needs a lot of manual marking on the images of the construction site; In three independent projects, the team finally marked more than 20 thousand images, which took about 240 working hours; An alignment error occurred when aligning the BIM model with the site point cloud; Some blind spots exceed 0.15m, which means manual intervention and maintenance are needed.

I found that the project manager showed mixed feelings about the automated building tools; Experienced workers tend to trust their intuition rather than software, and they are unwilling to fully accept the resource allocation plan proposed by the system; Because of this dependence on self-judgment, the actual adoption rate has dropped below 70% in some aspects.

3.3.2 Future Research Directions and Model Optimization Recommendations

At present, the training data are mainly from residential and commercial projects using three-frame shear wall structure, and it is not clear to what extent this method can be applied to other combinations (such as steel structures and precast concrete structures).

However, it is found that the actual progress of the project often changes gradually with the passage of time, and the dynamic adjustment method of λ will be considered in the future work, which is helpful to allocate automatic weight according to the recent change degree. It is worth noting that the strategy generation module provides man-machine cooperation settings, and most of the current system output is driven by algorithms, but in the future version, a manual input interface will be added, which uses a rule-based method to input the field experience directly accumulated by operators into the optimization model, which will eventually lead to mixed intelligent decision-making.

Looking into the future, building a lightweight deployment solution is undoubtedly another area

that needs work; At present, the system relies heavily on local servers and private networks, laying a solid foundation for the hardware cost of small projects; We will focus on cloud-based settings to reduce these initial obstacles; In order to reduce the response time, the lean planning engine is no longer used; On the contrary, the system combines the event-based method and the pre-arranged real-time alarm method, which helps to shorten the emergency response time to less than 15 minutes.

4. Conclusions

In this study, we set out to establish a real-time early warning and dynamic monitoring system for project progress, which is basically a combination of digital and BIM; Infrastructure consists of perception layer, transport layer, data, business logic and applications, which collect, process and collect data from multiple locations; When the prediction model based on LSTM is introduced into three experiments, the average absolute error is 1.51 days and the average absolute error is about 4.87%.

The dynamic threshold method based on weighted moving average shows an alarm accuracy of 88.95% and an alarm rate of 86.93%, which is 19.6 percentage points higher than the old fixed threshold method. In terms of scheduling, the multi-objective optimization algorithm successfully reduced the deviation of average duration by 59.45%, reduced the deviation of the whole project from 8.3% before deployment to 3.1% in management, and the average response time of the system was 45.2 minutes, which seemed to meet the daily management requirements well.

This work shows the practical application of digital twin technology in project schedule management, which is helpful to establish a comprehensive method from deviation detection to decision control. It seems that the future research will need to expand and test different types of structural project models, accurately adjust the adaptive threshold setting, and find a way to create a better acceptance control scheme through the cooperation between man-machine teams.

References

- [1] Liu X, Jiang D, Tao B, Xiang F, Jiang GZ, Sun Y, Kong JY, Li GF. A systematic review of digital twin about physical entities, virtual models, twin data, and applications. *Advanced Engineering Informatics*, 2023, 55: 101876. DOI:10.1016/j.aei.2023.101876
- [2] Jia WJ, Wang W, Zhang ZZ. From simple digital twin to complex digital twin part II: Multi-scenario applications of digital twin shop floor. *Advanced Engineering Informatics*, 2023, 56: 101915. DOI:10.1016/j.aei.2023.101915

- [3] Hwang J, Lim H, Lim J. Reducing uncertainty of building shape information in urban building energy modeling using Bayesian calibration. *Sustainable Cities and Society*, 2024, 116: 105895. DOI:10.1016/j.scs.2024.105895
- [4] Yang L, Chun Q, Zhang CW, Sun XL, Wang CH. Research on the Parametric Generation Method of Model with Multi-Information for the Wooden Architectural Heritage. *International Journal of Architectural Heritage*, 2025, 19(10): 2041-2066. DOI:10.1080/15583058.2024.2386013
- [5] Zhang H, Yan JW, Yang J, Meng W, Chen SJ. Two-stage point cloud registration using multi-scale edge convolution for digital twin-based bridge construction progress monitoring. *Automation in Construction*, 2025, 178: 106415. DOI:10.1016/j.autcon.2025.106415
- [6] Deng R, Li CE. Digital Intelligent Management Platform for High-Rise Building Construction Based on BIM Technology. *International Journal of Advanced Computer Science and Applications*, 2022, 13(12): 1057-1067.
- [7] Xiang L, Bai Y, He KX. BIM Reliability Prediction Method for Construction Schedule of Prefabricated Hollow Floor Based on Heterogeneous Data Fusion. *Journal of Structural Design and Construction Practice*, 2025, 30(2): 04025017. DOI:10.1061/JSDCCC.SCENG-1612
- [8] Du C, Wen Y, Ren LJ. Application of BIM model based on improved region growth algorithm in building reinforcement and renovation. *Archives of Civil Engineering*, 2024, 70(3): 445-457. DOI:10.24425/ace.2024.150994
- [9] Kong B, Jeong W. Development of an FMI-based data model to support a BIM-Integrated building performance analysis framework. *Buildings*, 2025, 15(17): 3200. DOI:10.3390/buildings15173200
- [10] Yin S. [10] Yin S. A construction schedule management method of large-scale construction project based on BIM model. *International Journal of Critical Infrastructures*, 2023, 19(2): 140-153. DOI:10.1504/IJCIS.2023.130456
- [11] Uslaender T, Baumann M, Boschert S, Rosen R, Sauer O, Stojanovic L, Wehrstedt JC. Symbiotic Evolution of Digital Twin Systems and Dataspaces. *Automation*, 2022, 3(3): 378-399. DOI:10.3390/automation3030020
- [12] Chen Q, Sheng N. Application of machine learning algorithm in stadium engineering building information model management system. *Mobile Information Systems*, 2022, 2022: 8454443. DOI:10.1155/2022/8454443
- [13] Tao F, Xiao B, Qi QL, Cheng JF, Ji P. Digital twin modeling. *Journal of Manufacturing Systems*, 2022, 64: 372-389. DOI:10.1016/j.jmsy.2022.06.015
- [14] Wei W, Lu YJ, Zhong T, Li PX, Liu B. Integrated vision-based automated progress monitoring of indoor construction using mask region-based convolutional neural networks and BIM. *Automation in Construction*, 2022, 140: 104327. DOI:10.1016/j.autcon.2022.104327
- [15] Wu SZ, Hou L, Zhang GM, Chen HS. Real-time mixed reality-based visual warning for construction workforce safety. *Automation in Construction*, 2022, 139: 104252. DOI:10.1016/j.autcon.2022.104252
- [16] Akin S, Gursel Dino I, Savas Sargin A. Heritage building information modelling for conservation of 20th century modernist architecture. *METU Journal of the Faculty of Architecture*, 2022, 39(1): 1-22. DOI:10.4305/METU.JFA.2022.1.1
- [17] Zhang YT. Safety management of civil engineering construction based on artificial intelligence and machine vision technology. *Advances in Civil Engineering*, 2021, 2021: 3769634. DOI:10.1155/2021/3769634
- [18] Deng H, Ou ZB, Deng YC. Multi-angle fusion-based safety status analysis of construction workers. *International Journal of Environmental Research and Public Health*, 2021, 18(22): 11815. DOI:10.3390/ijerph182211815
- [19] Alaloul WS, Qureshi AH, Musarat MA, Saad S. Evolution of close-range detection and data acquisition technologies towards automation in construction progress monitoring. *Journal of Building Engineering*, 2021, 43: 102877. DOI:10.1016/j.jobe.2021.102877
- [20] Li DR, Yu WB, Shao ZF. Smart city based on digital twins. *Computational Urban Science*, 2021, 1(1): 4. DOI:10.1007/s43762-021-00005-y
- [21] Song HR, Yu H, Xiao DL, Li YX. Real-time warning model of highway engineering construction safety based on Internet of Things. *Advances in Civil Engineering*, 2021, 2021: 6696014. DOI:10.1155/2021/6696014
- [22] Zhang CY, Arditi D. Advanced progress control of infrastructure construction projects using terrestrial laser scanning technology. *Infrastructures*, 2020, 5(10): 83. DOI:10.3390/infrastructures5100083
- [23] Zhang YY, Kang K, Lin JR, Zhang JP, Zhang Y. Building information modeling-based cyber-physical platform for building performance monitoring. *International Journal of Distributed Sensor Networks*, 2020, 16(2): 1550147720908170. DOI:10.1177/1550147720908170
- [24] Di Barba P, Galdi R, Mognaschi M E, et al. Special Issue on electromagnetic fields in mechatronics, electrical and electronic engineering. *International Journal of Applied Electromagnetics and Mechanics*, 2024, 76(1-2): 1-2.10.3233/jae-249004
- [25] Zhang J, Li T, Liu-Henke X. Adaptive multi-objective resource allocation for cooperative control of networked agents in cyber-physical systems. *2025 8th International Conference on Electronics Technology (ICET)*. IEEE, 2025: 1-6.10.1109/icet64964.2025.11103246